Nonempirical phase equilibria in the W-Mo-Cr system

R. McCormack and D. de Fontaine
Department of Materials Science and Mineral Engineering, University of California at Berkeley, Berkeley, California 94720

C. Wolverton
National Renewable Energy Laboratory, Golden, Colorado 80401

G. Ceder
Department of Materials Science, Massachusetts Institute of Technology, Cambridge, Massachusetts 02139
(Received 6 June 1994)

The solid-state portion of the W-Mo-Cr phase diagram is computed without the use of empirically adjustable parameters. The phase diagram is calculated using the bcc tetrahedron approximation of the cluster variation method (CVM) formulated with an independent set of multisite correlation functions. A set of volume-independent effective cluster interactions (ECI's) are used to parametrize the configurational energetics of the system; they are obtained using the method of direct configurational averaging based on a tight-binding, linearized muffin-tin-orbital Hamiltonian. The nearest- and next-nearest-neighbor pair ECI's are found to be dominant and indicate clustering tendencies for all binary systems (W-Mo, W-Cr, and Mo-Cr), consistent with experiment; triplet and higher-order pair interactions are significantly smaller. The ternary phase diagram for W-Mo-Cr is analyzed using twelve ECI's within the bcc tetrahedron, and while there is no experimental data for this ternary system, the results are quite encouraging even though transition temperatures on the binary edges are overestimated. The latter discrepancy is most likely due to the neglect of elastic relaxations driven by the large size mismatch of the constituent elements or to the neglect of vibrational contributions to the free energy.

INTRODUCTION

A knowledge of the phase behavior of materials is not only of scientific interest, but also of interest to the engineers who design materials. A survey of commonly used engineering materials would reveal most systems (alloys) to be multicomponent, i.e., mixtures of two or more elements. The phase behavior of binary systems has been well studied experimentally, but the same cannot be said for ternary or higher-order systems. The simplest reason for this is the "combinatorial explosion" in the number of different systems that can exist as the number of elements in the system increases. Hence, an exhaustive experimental study of even ternary phase equilibria is most likely an unrealistic goal. It would be advantageous if theoretical methods could be brought to bear on this problem, specifically methods that start from the atomic numbers of the constituent elements only. Theorists could then assist experimentalists in locating systems that might possess the desired phase behavior. Up to this point, the majority of theoretical studies have been limited to binary systems,[1-3] for which experimental data is already available. The real payoff in developing methods to determine phase behavior nonempirically comes when these methods are applied to ternary and higher-order systems.

The typical methodology in performing theoretical studies of phase equilibria involves using a generalized Ising model, where one studies substitutional disorder on a given Ising lattice by the use of various statistical mechanical techniques, e.g., the cluster variation method (CVM),[2,4] Monte Carlo simulations,[5] or transfer-matrix methods.[6] In *ab initio* approaches, input to the statistical-mechanical analysis comes from quantum-mechanical calculations, which rely on the atomic numbers for the system of interest. In phenomenological approaches, the input to the statistical-mechanical calculations is usually obtained by using various experimental data to fit the parameters used in the Ising model. The latter approach can provide interesting results, but one might argue that it is primarily a fitting procedure, which does not necessarily yield any insight into the physics involved in the problem at hand. In addition, it relies on the existence of experimental data (i.e., phase diagrams) in order to perform computations; clearly, this approach is of limited usefulness in studies of ternary (or higher-order) phase equilibria where such data is difficult and time consuming to obtain.

Studies of finite-temperature ternary phase equilibria to this point have been predominantly phenomenological in nature,[7-13] with the remainder of analyses being either based on prototype systems[14-19] or on select systems where input to the statistical mechanics was derived from quantum-mechanical total-energy calculations.[20-23] Most studies (prototype or otherwise) have used short-ranged correlations to study order-disorder phenomena on the fcc and bcc lattices. It does not appear that any ternary studies have been done on the hcp lattice or any other more complex structure. Virtually all of the aforementioned studies used a cluster probability formulation of the CVM to compute phase equilibria, a method that becomes somewhat intractable as the range of corre-

0163-1829/95/51(22)/15808(15)/$06.00

lations is increased.

In the present analysis, we utilize the cluster expansion formulation of the CVM for ternary systems based on the seminal work of Sanchez, Ducastelle, and Gratias (SDG).[24] Such a formulation of the ternary CVM should allow CVM calculations for complex systems, where the more commonly used cluster probability method is unwieldy. The cluster-expansion development of the ternary CVM is tailor made to receive input from quantum-mechanical calculations based on a knowledge of only the constituent elements of the alloy. This approach is used herein to examine finite-temperature solid-solid phase equilibria in the W-Mo-Cr system, a bcc-based ternary system in which phase separation is observed in all three binary phase diagrams. The motivation for studying this system is twofold: (1) the system has three transition metal elements that possess the same number of d electrons and (2) the constituent binary systems do not exhibit compound formation. The former point is of interest, since the configurational energy in the present analysis will be based on quantities determined by a real-space *nonempirical* tight-binding (TB) method. Many TB calculations for transition metals only distinguish elements based on the number of d electrons they possess ("canonical d-band" analyses, diagonal disorder only),[2,25] and thus one might expect there to be no preference for ordering or phase separation in the W-Mo-Cr system.[2] This cannot be the case given the experimentally observed behavior of the binary systems. The present TB method uses an expanded basis set (s, p, and d-electrons) and also allows for the presence of off-diagonal disorder (ODD) in the Hamiltonian. Thus, we expect these factors (particularly ODD) to have a dominant effect on the ordering or clustering tendencies in W-Mo-Cr. The second motivation is less subtle and more practical in nature: simplicity of the binary systems is a benefit since one generally wishes to choose a system that should be amenable to a nonempirical treatment. The basic intent of this paper is to show the viability of nonempirical methods in the determination of ternary phase equilibria; hence any trial system chosen should not be expected to possess pathological behavior. The W-Mo-Cr system satisfies this criterion, yet despite its apparent simplicity, the authors hope to demonstrate the difficulty in accurately treating its phase behavior.

I. FORMALISM

The formalism associated with the computation of phase diagrams is quite extensive, and an exhaustive review of all of the relevant methods would not be instructive. The following section will present a brief overview of the methods used in the computation of the W-Mo-Cr phase diagram: generalized Ising models and the cluster expansion for functions of configuration, parametrization of configurational energetics, and the cluster variation method (CVM). For the sake of brevity, the majority of the formalism will not be presented; references which contain more detailed information will be provided in the text for the interested reader.

A. Generalized Ising models and the cluster expansion

One method for treating substitutional (dis)order in alloys is to map the alloy problem onto a generalized Ising model, where atomic species are assumed to be associated with the sites of a given Ising lattice. In this model, no dynamic displacements of atoms away from lattice sites are allowed; only configurational effects are examined. The occupation of each site in this lattice is then represented by a pseudospin variable (site occupation operator) σ_i. For a binary alloy, σ_i can take the values $+1$ or -1 if site i is occupied by an A or B atom. Similarly, in a ternary alloy, one can represent site occupation by $+1$, 0, or -1 if site i is occupied by an A, B, or C atom. The configuration in the alloy can then be represented by a vector, which specifies the occupation of each site $\boldsymbol{\sigma}=\{\sigma_1,\sigma_2,..,\sigma_N\}$. A paper by Sanchez, Ducastelle, and Gratias[24] (SDG) showed that *any* given function of configuration $f(\boldsymbol{\sigma})$ can be written as a linear expansion in terms of a set of functions that depend on the configuration $\boldsymbol{\sigma}$. For example, when $f(\boldsymbol{\sigma})$ is the energy of a configuration of atoms on the lattice, the expansion of SDG allows this energy to be written as a sum of "cluster energies," where the *cluster* refers to a collection of lattice sites, (e.g., a pair or triplet of sites). The expansion is thus commonly referred to as the *cluster expansion.* A detailed discussion of the specific application of the cluster expansion to ternary systems can be found in Wolverton and de Fontaine.[26]

For a ternary alloy, we need to be able to describe functions that depend on the occupation of the lattice sites by three species (A,B,C). As a starting point, consider a function that depends on the occupation of a single site i (e.g., the atomic number of the species on that site). In order to *completely* describe such a function, three separate functions of the site occupation operator σ_i are necessary. These functions $\chi_{s_i}(\sigma_i)$ ($s_i=0,1,2$) are then distinguished by a label s_i; numerous choices are possible for the exact form of these functions.[24,26,27] If we then wish to describe functions that depend on the occupation of a *cluster* of lattice sites (α), we take products of these "point" functions $\chi_{s_i}(\sigma_i)$ to yield the so-called *cluster functions* $\Phi_\alpha^{(s)}$:

$$\Phi_\alpha^{(s)}(\boldsymbol{\sigma})=\chi_{s_1}(\sigma_1)\chi_{s_2}(\sigma_2)\cdots\chi_{s_\alpha}(\sigma_\alpha)\ . \tag{1}$$

The subscript $\alpha=\{p_1,p_2,\ldots,p_\alpha\}$ specifies the sites of the lattice that comprise cluster α, and the superscript $s=\{s_1,s_2,\ldots,s_\alpha\}$ ($s_i=0,1,2$) is the function label. Hereafter, the function label (s) will be referred to as the *decoration* of cluster α, not to be confused with the possible configurations of atomic species on α. For an arbitrary function of configuration $f(\boldsymbol{\sigma})$, the most general ternary cluster expansion is then written as

$$f(\boldsymbol{\sigma})=\sum_\alpha\sum_s f_\alpha^s\Phi_\alpha^{(s)}(\boldsymbol{\sigma})\ , \tag{2}$$

where $f_\alpha^{(s)}$ are referred to as the *cluster-expansion coefficients* (CEC's). If the functions $\chi_{s_i}(\sigma_i)$ correspond to discrete Chebychev polynomials, then one recovers the

original formulation of SDG. In this development, one can actually write down a definition for the CEC's by using certain properties of the expansion.[24] If one instead chooses to use a simpler set of functions such as $\{1,\sigma_i,\sigma_i^2\}$ for $\chi_{s_i}(\sigma_i)$,[27,28] there is no simple definition for CEC's. However, any set of $\chi_{s_i}(\sigma_i)$ that are viable can be related via a linear transformation to any other set of $\chi_{s_i}(\sigma_i)$.[26,29] This property allows either cluster functions or expansion coefficients to be computed with respect to any viable choice of $\chi_{s_i}(\sigma_i)$.

The expansion coefficients in Eq. (2) possess the symmetry of the Ising lattice under consideration.[30] Thus, all CEC's are equivalent for decorated clusters (specified by α *and* s) that can be transformed into one another by symmetry operations of the space group of the lattice. Such a set of CEC's are said to be in the same crystallographic *orbit*, a term which will hereafter be used to denote a set of objects that are symmetry equivalent. Application of the space-group symmetry to the cluster expansion allows one to group terms in Eq. (2) and then rewrite the expansion in terms of a set of *lattice-averaged* cluster functions (LACF's) (indicated with an overbar):

$$f(\sigma)=\sum_{\alpha}\sum_{s} m_{\alpha}^{(s)} f_{\alpha}^{(s)} \overline{\Phi_{\alpha}^{(s)}}(\sigma) \ . \tag{3}$$

Summations in Eq. (3) include only symmetry-distinct clusters α and decorations of those clusters (s). The multiplicities $m_{\alpha}^{(s)}$ correspond to the number of clusters of type α with decoration s that can be associated with a given lattice site. This quantity is simply the number of α clusters per lattice point (m_{α}) multiplied by the number of equivalent decorations of type s (m_s) on cluster α (i.e., $m_{\alpha}^{(s)}=m_{\alpha}m_s$). It should be pointed out that the cluster expansion equivalent to Eq. (3) in Ref. 26 does not use the same convention for the multiplicities; in that paper, summation over the index s includes *all* decorations on the cluster α, not just those that are symmetry distinct.

The cluster expansion in Eq. (2) is *exact* if one includes all 3^N terms in the expansion, although in practice this is clearly impossible. The expansion is truncated at a point dictated by the problem at hand, and in most cases this makes the problem tractable. The convergence of the expansion is an issue that has been discussed in the context of binary systems to a great extent,[31–33] but there has been very little discussion of convergence in ternary cluster expansions, primarily due to the limited extent to which the expansion has been used. Some discussion of the convergence of ternary expansions can be found in Wolverton and de Fontaine.[26]

B. Parametrization of configurational energetics

When the function of configuration in Eq. (3) is the energy of a configuration of atoms, the CEC's are referred to as *effective cluster interactions* (ECI's). The interface between quantum and statistical mechanics for the computation of phase equilibria is provided primarily by these ECI's. Numerous methods exist[1,3,34–36] to compute effective cluster interactions, each of which has its own set of advantages and disadvantages. The approach that has been used in the present work is the method of direct configurational averaging[33,37] (DCA) in which the ECI's are computed *directly* from the definition provided by the cluster expansion based on *Chebychev* polynomials. The linear independence of the basis functions allows for a transformation of the interactions from this Chebychev representation into potentially more convenient basis sets (e.g., $\{1,\sigma_i,\sigma_i^2\}$).[26,29] In the present formulation of the DCA, the primary contribution to the interactions comes from the sum of one-electron eigenvalues (the "band energy"). The DCA is a real-space technique based on a tight-banding (TB) Hamiltonian with parameters usually obtained by casting a linearized-muffin-tin-orbital (LMTO) Hamiltonian into TB form using the prescription of Andersen and Jepsen.[38] The ECI's are expressed as diagonal matrix elements of the one-electron Green's function, which are computed using the recursion method.[33,37] A detailed description of the DCA and calculations based on the DCA can be found in Ref. 33. The major advantage of the DCA is that it computes interactions based on an *exact* definition, which allows ECI's to be computed independently of one another. The ECI's would not be independent if one were to use methods based on the ideas of Connolly and Williams.[34] One disadvantage of the DCA is that at this point one seems to be limited to using a TB representation, which may not always provide the most accurate descriptions of the electronic structure of the alloy.

The specific form that ternary Chebychev ECI's take can be determined using the cluster expansion.[26] The definitions become somewhat complex, and, in the case of pair interactions, it is no longer possible to assess by examination the ordering tendencies of a given alloy system. In contrast, the interpretation of binary pair ECI's is straightforward. For a binary alloy, the pair ECI for sites p and p' takes the following form:[32,39]

$$V_{pp'}=\tfrac{1}{4}(E_{AA}+E_{BB}-E_{AB}-E_{BA}) \ . \tag{4}$$

Each term E_{IJ} in Eq. (4) represents the *average* energy of all *binary* configurations with sites p and p' filled by atoms I and J, respectively. The interpretation of the ECI in Eq. (4) is quite simple: when $V_{pp'}>0$ (<0), the system prefers unlike (like) atoms on sites p and p'. Hence, if p and p' connect nearest-neighbor (NN) sites, the system will produce ordered compounds if $V_{pp'}>0$ and will phase separate if $V_{pp'}<0$. For ternary alloy pair ECI's, there are *three* distinct ternary pair interactions for $\alpha=\{p,p'\}$, which we will call $V_{pp'}^{(11)}$, $V_{pp'}^{(12)}$, and $V_{pp'}^{(22)}$, the superscript in brackets denoting the decoration of the cluster of sites. Each of these ECI's corresponds to a slightly different linear combination of configurationally averaged pair energies. In that sense, the interactions are not very different in spirit from the expression in Eq. (4). The exact expressions for these interactions with respect to the Chebychev formulation of Eq. (2) are as follows:[26]

$$V_{pp'}^{(11)}=\tfrac{1}{6}(E_{AA}+E_{CC}-E_{AC}-E_{CA}) \ , \tag{5}$$

$$V_{pp'}^{(12)}+V_{pp'}^{(21)}=\frac{\sqrt{3}}{9}(-E_{AA}+E_{AB}+E_{BA}-E_{BC}-E_{CB}+E_{CC}) \ , \tag{6}$$

$$V_{pp'}^{(22)} = \tfrac{1}{18}(E_{AA} - 2E_{AB} + E_{AC} - 2E_{BA} + 4E_{BB} - 2E_{BC} + E_{CA} - 2E_{CB} + E_{CC}) \ . \quad (7)$$

Now, each term E_{IJ} in Eqs. (5)–(7) represents the average energy of all *ternary* configurations with sites p and p' filled by atoms I and J, respectively. In Eq. (6), we have written the sum of $V_{pp'}^{(21)}$ and $V_{pp'}^{(12)}$, since it yields a more useful expression, which can be recast in terms of pseudobinary interactions. In the case where the points p and p' are symmetry equivalent, these two interactions should be equal in the limit of averaging over all 3^{N-2} configurations. Since the DCA averages over a finite number of configurations, we do not in general expect the two to be exactly equivalent. Therefore, in the cluster expansion of the energy, we simply use Eq. (6) and divide by two to obtain the $V_{pp'}^{(12)}$ ECI.

A comparison of Eqs. (4) and (5) shows that the ternary interaction $V_{pp'}^{(11)}$ is nothing more than a "pseudobinary" interaction with a slightly different normalization. This interaction is pseudobinary in the sense that the definition has the same form as Eq. (4) (a binary definition), but the configurational averaging for the energies E_{IJ} is performed with respect to a ternary medium. It is actually possible[26] to rewrite the ECI's in Eqs. (5)–(7) as three pseudobinary pair ECI's: $W_{pp'}^{AB}$, $W_{pp'}^{AC}$, and $W_{pp'}^{BC}$. Each of these $W_{pp'}^{IJ}$ interactions then have the same interpretation in terms of ordering vs clustering tendencies as the binary alloys ($W_{pp'}^{IJ} > 0$ = ordering for binary system IJ, $W_{pp'}^{IJ} < 0$ = clustering for binary system IJ). This transformation allows for a simpler assessment of the relative ordering tendencies in the binary edge systems (AB, AC, and BC) using the ternary pair interactions. Note that definitions similar to those in Eqs. (5)–(7) can be written for triplet and higher-order ECI's,[26] although it is unclear whether a transformation of these ECI's to pseudobinary form is possible.

C. The cluster variation method

The cluster variation method[4] (CVM) is a statistical-mechanical technique for approximating the configurational entropy of systems of interacting species (in this case, the atoms of an alloy). The fundamental approximation of the CVM resides in assuming that species are only directly correlated over a given range specified by choosing one or more *maximal clusters* (α_M).[40,41] The configurational entropy is then written as a sum of cluster entropies associated with the probabilities of observing various configurations (J) of atoms on clusters (α) of lattice sites (the so-called *cluster probabilities* X_α^J). There are primarily two methods of constructing a free energy based on the CVM. In the first (see, for example, Ref. 18), one writes both the energy and entropy in terms of the cluster probabilities (a dependent set of variables). In the second approach, one expands the cluster probabilities according to Eq. (3) and writes the CVM free energy as a functional of independent *multisite correlation functions* ($\xi_\alpha^{(s)}$). The correlation functions are just the thermodynamic average of the LACF's presented in Sec. I A. All ternary CVM studies to this point except those in Refs. 20 and 23 have used a cluster probability formulation of the ternary CVM. The more general approach using a cluster expansion for the probabilities (hereafter referred to as the cluster expansion formulation of the CVM) provides for greater flexibility in terms of both the computation of ECI's and in the level of complexity that can be treated.

The cluster expansion formulation of the CVM for ternary systems is essentially identical to the formulation for binary systems, which can be found in Ref. 42. The CVM Helmholtz free energy per lattice point of a given ternary structure can be written as follows:

$$f_{\rm CVM} = \sum_\alpha \sum_s m_\alpha^{(s)} V_\alpha^{(s)} \xi_\alpha^{(s)} + k_B T \sum_\beta^{\alpha_M} \gamma_\beta \sum_J X_\beta^J \ln X_\beta^J \ , \quad (8)$$

$$X_\beta^J = \frac{1}{\rho^0} \sum_{\gamma \subseteq \beta} \sum_s \nu_{\beta\gamma}^J \xi_\gamma^{(s)} \ . \quad (9)$$

The first term in Eq. (8) corresponds to the configurational energy based on the effective cluster interactions $V_\alpha^{(s)}$. The second term represents the configurational entropy, and the sum contains all clusters up to and including the maximal cluster(s). In the energy expression, the sum need only contain a subset of these clusters (it cannot contain a superset, i.e., clusters outside the maximal cluster, without introducing additional approximations to the CVM free-energy expression).[43] The coefficients γ_β are geometrical quantities commonly referred to as Kikuchi-Barker coefficients[2,24] and are the same for a given lattice, regardless of the number of components. The cluster probabilities (X_β^J) in their cluster-expanded form are given in Eq. (9) as a sum over all subclusters of cluster β, where ρ_0 is a normalization factor and $\nu_{\beta\gamma}^J$ are the so-called V-matrix coefficients (determined by group theoretical methods). A discussion of the V-matrix in ternary systems can be found in Ceder *et al.*[44]

Given an expression for the CVM free energy of a phase, one chooses a suitable starting point for the correlation functions (usually a superposition approximation) and then obtains their equilibrium values by minimizing the free energy. In the present formulation, minimization is performed with a multivariable Newton-Raphson method, which allows for the treatment of relatively large sets of correlation functions. Once the free energy is obtained for the disordered phase and all other phases of interest (the latter usually determined by a ground-state search[44] based on the interactions $V_\alpha^{(s)}$), one can then build the phase diagram using standard techniques such as common-tangent construction or location of grand-potential intersections.[17,18]

II. COMPUTATION OF THE W-Mo-Cr PHASE DIAGRAM

The method of direct configurational averaging (DCA) described in Sec. I is used to compute ECI's and the solid-state portion of the phase diagram for the W-Mo-Cr system. Each of the constituent elements in W-Mo-Cr possess the bcc structure, which means that calculations need only be performed on the bcc lattice. The experi-

mental equilibrium molar volumes of W, Mo, and Cr are 9.443, 9.601, and 7.274 cm^3 mol^{-1}, respectively, indicating a huge size mismatch between (W, Mo) and Cr. The W-Cr and Mo-Cr binary phase diagrams exhibit miscibility gaps with maxima at 1677 and 880°C, respectively,[45] while W-Mo shows complete solid solubility in the range of temperatures studied with indications of a possible low-temperature miscibility gap. One theoretical study[46] of the phase diagrams for these three binary systems agrees quite well with experiment and indicates the presence of a miscibility gap in W-Mo at very low temperature, as anticipated. An additional theoretical study of the Mo-Cr system[47] also agreed with experiment (see Sec. II C for a more extended discussion of Refs. 46 and 47). No experimental data appears to exist for ternary alloys in this system.

A. Effective cluster interactions

LMTO calculations in the atomic-sphere-approximation (ASA) are performed at several volumes for all three of the pure elements. These calculations are performed scalar relativistically (i.e., without spin-orbit interactions) and include the combined corrections[48] to the ASA, while muffin-tin corrections to the ASA are *not* included. Calculations are not performed with spin polarization, even though Cr has an antiferromagnetic ground state. It seems justifiable to neglect spin polarization, since the Néel temperature for Cr is 308 K, a temperature low enough so that one expects magnetism to play an insignificant role in high-temperature phase equilibria. In addition, it is known that the local density approximation (LDA) does not treat magnetism in Cr properly, predicting a paramagnetic ground state.[49,50] The exchange-correlation potential of Von Barth and Hedin[51] is used, and the basis set contains orbitals with $l=0$, 1, and 2. All total-energy calculations are converged to within 0.1 mRy/atom with 165 **k** points sampled in the irreducible wedge of the Brillouin zone; energy computations are performed at a series of volumes for each element, and the resulting total energies are fit to a third-order polynomial in volume. Equilibrium quantities are determined based on the cubic polynomial equation of state. The predicted equilibrium volumes, lattice constants, and bulk moduli for W, Mo, and Cr are given in Table I. Agreement with experimental results is standard for calculations based on the LDA for W and Mo; the large error in volume and bulk modulus for Cr are due to the incorrect treatment of magnetism.

Effective cluster interactions for W-Mo-Cr system are computed using the DCA. Slater-Koster (SK) TB parameters [on-site energies, NN and next-nearest-neighbor (NNN) hopping integrals for *s*, *p*, and *d* orbitals] are extracted from pure-element LMTO calculations[38] at two different volumes: (1) all elements at the volume of an *equiatomic* alloy given by Vegard's law ($\Omega_0=8.774$ cm^3 mol^{-1}) and (2) each element at its *equilibrium* volume. The sets of interactions computed at each of these volumes are hereafter referred to as sets SK(I) and SK(II), respectively. The on-site energies and hopping integrals for the two volumes are given in Table II. It is clear from an examination of this table that the TB parameters are quite sensitive to the volume used in the LMTO calculations. The ECI's calculated using the DCA are also sensitive to these parameters, although one can make some qualitative assessments about what set of parameters are more reasonable (see Sec. II C).

DCA calculations are performed using the SK parameters in Table II. The on-site energies of Mo and Cr are shifted to maintain configurationally averaged charge neutrality.[33,37] Hopping matrix elements between elements of different types are obtained by taking the geometric mean[52] of pure-element hopping integrals [$\beta_{IJ}=(\beta_{II}\beta_{JJ})^{1/2}$; I,J = W, Mo, Cr]. In order to determine the shifts for Mo and Cr, calculations are performed using ten levels of recursion on the TB Hamiltonian (five levels exact), which yields a recursion cluster of roughly 1000 atoms; results are averaged over 8 and 20 configurations of the atoms on these sites with little or no change in the results. Shifts and Fermi levels for the two sets of SK parameters [SK(I) and SK(II)] are given at the foot of Table II. The interaction clusters are the first- through fifth-NN pairs and the triplet containing two NN and one NNN pairs. For both sets SK(I) and SK(II), a total of 23 different ECI's are computed with the DCA, 15 based on pair interactions ($V^{(ij)}_{2,n}$, $n=1-5$) and the other eight computed for triplet interactions ($V^{(ijk)}_{3,1}$). The notation $V^{(s)}_{n,m}$ will occasionally be used for ECI's $V^{(s)}_{\alpha}$, where n indicates the number of points in the cluster α and m gives a relative size or point separation.[33] It is assumed that quadruplet interactions will be small and can be neglected at this stage in the calculations. The various interaction clusters are shown in Fig. 1; for each one of these clusters, there are multiple ECI's which have different decorations of the interaction cluster (see Secs. I A and I B). The distinct decorations, cluster multiplicities ($m^{(s)}_{\alpha}$) and Kikuchi-Barker coefficients (γ_{β}) are given in Table III. Information for the third- through fifth-nearest-neighbor pairs is omitted from Table III, since these clusters will not be included in CVM calculations.

TABLE I. Equilibrium volumes, lattice constants, and bulk moduli for W, Mo, and Cr as determined by LMTO-ASA calculations. Calculations are performed at a series of volumes and then fit to a third-order polynomial in volume. The agreement between theory and experiment (indicated in parentheses) for W and Mo is quite good, but the volume (bulk modulus) for Cr is predicted to be too small (large) compared with experiment.

Element	Volume (cm^3 mol^{-1})	Lattice constant (Å)	Bulk modulus (mbar)
W	9.784 (9.443)	3.190 (3.165)	3.1856 (3.232)
Mo	9.631 (9.601)	3.173 (3.147)	2.7880 (2.725)
Cr	6.869 (7.274)	2.835 (2.885)	2.9256 (1.901)

TABLE II. Pure-element tight-binding parameters for W, Mo, and Cr extracted from LMTO-ASA calculations for each element. On-site energies (ε_i) and nearest- and next-nearest-neighbor hopping integrals (β_{NN} and β_{NNN}) are given for two different sets of LMTO calculations. In case I [SK(I)] (columns 1–3), LMTO calculations are performed for the elements at the *equiatomic* volume given by Vegard's law ($\Omega_0 = 8.774$ cm^3 mol^{-1}). In case II [SK(II)], LMTO calculations are performed for each element at its *equilibrium* volume as determined by LMTO-ASA calculations. All SK parameters are in rydbergs. Shifts and Fermi levels indicate values of these quantities for DCA calculations based on each data set.

SK parameter	W(I)	Mo(I)	Cr(I)	W(II)	Mo(II)	Cr(II)
			ε_i			
s	0.3435	0.5347	0.2614	0.1891	0.3907	0.5731
p	1.5559	1.5680	1.0736	1.285	1.339	1.5312
t_{2g}	0.2810	0.1971	−0.0598	0.1630	0.1035	0.1197
e_g	0.2193	0.1460	−0.0815	0.1105	0.0591	0.0881
			β_{NN}			
$ss\sigma$	−0.1070	−0.1116	−0.0978	−0.0955	−0.1019	−0.1233
$pp\sigma$	0.4320	0.4295	0.3594	0.3866	0.3903	0.4474
$pp\pi$	−0.0659	−0.0655	−0.0548	−0.0590	−0.0595	−0.0682
$dd\sigma$	−0.1680	−0.1392	−0.0590	−0.1432	−0.1208	−0.0860
$dd\pi$	0.0810	0.0671	0.0284	0.0690	0.0582	0.0414
$dd\delta$	−0.0083	−0.0069	−0.0029	−0.0071	−0.0060	−0.0042
$sp\sigma$	0.2144	0.2184	0.1870	0.1916	0.1989	0.2343
$sd\sigma$	−0.1262	−0.1173	−0.0715	−0.1100	−0.1044	−0.0969
$pd\sigma$	−0.2622	−0.2380	−0.1418	−0.2290	−0.2113	−0.1908
$pd\pi$	0.0734	0.0666	0.0397	0.064 10	0.0591	0.0534
			β_{NNN}			
$ss\sigma$	−0.0327	−0.0349	−0.0422	−0.0366	−0.0382	−0.0335
$pp\sigma$	0.1523	0.1538	0.1763	0.1702	0.1692	0.1416
$pp\pi$	−0.008 20	−0.0083	−0.0095	−0.0092	−0.0091	−0.0076
$dd\sigma$	−0.0656	−0.00554	−0.0394	−0.0770	−0.0638	−0.0271
$dd\pi$	0.0134	0.0113	0.0081	0.0157	0.0131	0.0055
$dd\delta$	−0.0007	−0.0006	−0.0004	−0.0009	−0.0007	−0.0003
$sp\sigma$	0.0714	0.0742	0.0874	0.0800	0.0814	0.0697
$sd\sigma$	−0.0465	−0.0441	−0.0409	−0.0533	−0.0496	−0.0302
$pd\sigma$	−0.1008	−0.0930	−0.0840	−0.1154	−0.1048	−0.0624
$pd\pi$	0.0102	0.0094	0.0085	0.0116	0.0106	0.0063
Shift	0.000	0.038	0.251	0.000	0.0225	−0.02
E_F		0.1167			0.0362	

The results of the ECI calculations for SK(I) and SK(II) are given in Table IV; it should be emphasized that these interactions are computed with respect to the *Chebychev* basis set. The value of each ECI is the *mean* value of all of the ECI's computed for the number of configurations (N_{conf}) specified in the third and seventh columns of Table IV. In order to assess the accuracy of the configurational averaging process, the standard deviation of the average ECI (the second and sixth columns of Table IV) can be written in terms of the standard deviation in the set of ECI's (σ_{conf}).[33] For the calculation of ECI's using SK(I), ten levels of recursion are used with five levels computed exactly. Some tests showed that identical results can be obtained using only eight levels of recursion (three levels exact), so for calculations with SK(II), the latter is used. In all cases, the configurational averaging is performed in a medium with the equiatomic concentration; using such a concentration ensures the equivalence of concentration-dependent and -independent interactions.[32,39,53,54] Examination of the table of ECI's shows that for the NN and NNN pair ECI's, the deviation of the ECI's is quite small, indicating acceptable convergence with respect to configurational averaging. It should be noted that two groups of the triplet ECI's ($V_{3,1}^{(121)}$ and $V_{3,1}^{(211)}$; $V_{3,1}^{(212)}$ and $V_{3,1}^{(122)}$) are actually in the same decoration orbit, although the values of the ECI's for the (121) and (211) ECI's are different. The average

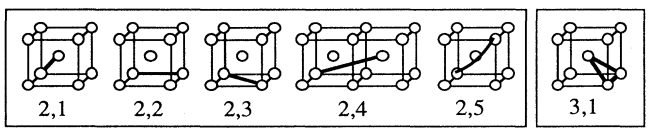

FIG. 1. bcc interaction clusters used in DCA calculations for the W-Mo-Cr system. The nth neighbor pair cluster are indicated $(2,n)$, and the first triplet cluster is shown as (3,1).

TABLE III. Information for the ternary cluster expansion on the bcc lattice. *Number:* indicates a label for the cluster function or corresponding interaction. *Cluster:* indicates the atomic sites, which make up the given cluster, relative to a conventional bcc unit cell with scaled coordinates, where (200) corresponds to the corner atom along x and (111) corresponds to the body center. *Decoration:* Corresponds to decoration of the cluster of sites indicated in the second column by the point functions; the order of the decoration corresponds to the order of presentation of the sites in the second column. The decorations in parentheses are all other decorations of the cluster α that are equivalent by symmetry. *Multiplicity* ($m_\alpha^{(s)}$): number of clusters of type α with decoration (s) per lattice point. *Kikuchi-Barker coefficients:* γ_β, equal for all cluster functions that share a common cluster α.

Number	Cluster (α)	Decoration (s)	$m_\alpha^{(s)}$	γ_B
1	Empty	None	1	
2	(000)	2	1	−1
3	(000)	1	1	−1
4	(000) (200)	22	3	3
5	(000) (200)	12 (21)	6	3
6	(000) (200)	11	3	3
7	(000) (111)	22	4	4
8	(000) (111)	12 (21)	8	4
9	(000) (111)	11	4	4
10	(000) (111) (200)	222	12	−12
11	(000) (111) (200)	221	12	−12
12	(000) (111) (200)	212 (122)	24	−12
13	(000) (111) (200)	211 (121)	24	−12
14	(000) (111) (200)	112	12	−12
15	(000) (111) (200)	111	12	−12
16	(000) (111) (200) (111)	2222	6	6
17	(000) (111) (200) (111)	2221 (2212,2122,1222)	24	6
18	(000) (111) (200) (111)	2211 (1122)	12	6
19	(000) (111) (200) (111)	2121 (1212, 1221, 2112)	24	6
20	(000) (111) (200) (111)	1211 (1112, 1121, 2111)	24	6
21	(000) (111) (200) (111)	1111	6	6

value is used for the representative interaction in the ground-state and CVM calculations. A ground-state analysis[44] within the range of the bcc tetrahedron is done with this set of ECI's, and it is found that no compounds form for this set of interactions, i.e., the ground states are simply the three pure elements. LMTO-ASA calculations of the formation enthalpies for a series of compounds are in agreement with this prediction, although compound formation enthalpies predicted with the DCA interactions [either SK(I) or SK(II)] are larger in magnitude (i.e., more positive).

All of the pair ECI's computed using SK(I) (LMTO calculations at Vegard's law equiatomic volume) and SK(II) (LMTO calculations at equilibrium volume of each element) are plotted as a function of pair separation in Figs. 2(a) and 2(b). It can be seen quite clearly that the NN pair ECI is the dominant one with the NNN pair ECI quite a bit smaller but still significant. All of the higher-order pair interactions are small compared with the NN and NNN ECI's. An examination of the triplet interactions in Table IV also reveals these triplets are all quite small compared to the NN pair ECI's. It is therefore expected that higher-order ECI's such as quadruplets would be insignificant, and neglecting these interactions is justified. The trends followed in the ECI's appear to be consistent with the trend observed in binary ECI calculations:[31–33] the ECI's decay in magnitude with respect to both separation of the points in the cluster and with number of points in the cluster. It is natural to ask whether, for a given cluster of sites, there is a systematic variation in the relative sizes of ECI's with different decorations of that cluster. For at least the pair ECI's, it appears that the magnitude of the ECI's for a given cluster of sites is inversely proportional to the number of terms in the definition of that ECI, i.e., $V_{pp'}^{(22)} < V_{pp'}^{(12)} < V_{pp'}^{(11)}$ for p and p' fixed. Similar behavior can be observed in the calculations of Wolverton *et al.*[26] for the pair ECI's in their study of three different ternary alloys. In addition, it appears that the rate of convergence with respect to cluster size (e.g., pair separation or number of sites in cluster) is relatively independent of cluster decoration. The foregoing discussion should not be taken as a general assessment of convergence of the ternary cluster expansion; additional studies need to be performed.

If we transform the NN pair ECI's for SK(I) and SK(II) into their pseudobinary representation,[26] we can assess the predictions made concerning the W-Mo-Cr system by the DCA in a straightforward way. The pseudobinary interactions for SK(I) [SK(II)] indicate phase separation for all three binary systems: $W_{\mathrm{NN}}^{\mathrm{WCr}} = -215$ (−35) meV, $W_{\mathrm{NN}}^{\mathrm{MoCr}} = -131$ (−20) meV, and $W_{\mathrm{NN}}^{\mathrm{WMo}} = -3.5$ (−1.6) meV. In order to gain an estimate of the transition temperature that will arise from these pseudobinary

TABLE IV. Effective cluster interactions (ECI's) for the W-Mo-Cr system computed using two different sets of Slater-Koster parameters [SK(I) and SK(II)]. Within each SK(i) block are given the configurationally averaged (CA) value of the interaction (in meV), the number of configurations (N_{conf}) that were averaged over in the DCA, the rms deviation of the value of the ECI (σ_{conf}), and the deviation ($\sigma_{\text{conf}}/R_{\text{conf}}$) in the CA value, where $R_{\text{conf}}=(N_{\text{conf}})^{1/2}$. The deviation in the CA value is a measure of the effect of configurational averaging; a small value of this quantity indicates relative convergence with respect to configurational averaging. Investigation of the table shows that for the NN pair ECI's (11, 12+21, and 22), the deviation in the mean value is small (1%) compared to the values of the interactions themselves.

	SK(I)				SK(II)			
Cluster	$V_\alpha^{(s)}$	N_{conf}	σ_{conf}	$\sigma_{\text{conf}}/R_{\text{conf}}$	$V_\alpha^{(s)}$	N_{conf}	σ_{conf}	$\sigma_{\text{conf}}/R_{\text{conf}}$
$V_{2,1}^{(11)}$	−144.415	20	2.4818	0.5549	−23.554	20	1.5641	0.3497
$V_{2,2}^{(11)}$	−19.290	20	2.0695	0.4627	−1.622	20	0.7656	0.1712
$V_{2,3}^{(11)}$	−1.322	10	0.6265	0.1981	0.847	10	0.3006	0.0950
$V_{2,4}^{(11)}$	0.548	10	0.3523	0.1114	0.724	10	0.1145	0.0362
$V_{2,5}^{(11)}$	2.025	10	1.0586	0.3348	0.572	10	0.9681	0.3061
$V_{2,1}^{(12+21)}$	−99.156	20	3.0870	0.6903	−13.842	20	1.2792	0.2860
$V_{2,2}^{(12+21)}$	−14.540	20	1.7877	0.3997	−2.296	20	0.5697	0.1274
$V_{2,3}^{(12+21)}$	−1.272	10	0.3396	0.1074	0.445	10	0.3719	0.1176
$V_{2,4}^{(12+21)}$	−0.039	10	0.2049	0.0648	0.184	10	0.1492	0.0472
$V_{2,5}^{(12+21)}$	2.137	10	0.9635	0.3047	0.630	10	0.4909	0.1552
$V_{2,1}^{(22)}$	−13.635	17	0.6956	0.1687	−1.755	20	0.3761	0.0841
$V_{2,2}^{(22)}$	−3.379	20	0.3223	0.0721	−0.325	20	0.0862	0.0193
$V_{2,3}^{(22)}$	−0.188	10	0.0793	0.0251	0.043	10	0.0779	0.0246
$V_{2,4}^{(22)}$	−0.057	10	0.0544	0.0172	0.026	10	0.0255	0.0081
$V_{2,5}^{(22)}$	0.487	10	0.2287	0.0723	0.139	10	0.1128	0.0357
$V_{3,1}^{(111)}$	0.472	10	0.3372	0.1066	0.138	10	0.1488	0.0471
$V_{3,1}^{(121)}$	0.250	10	0.1588	0.0502	0.121	10	0.0772	0.0244
$V_{3,1}^{(112)}$	0.336	10	0.1378	0.0436	0.094	10	0.0702	0.0222
$V_{3,1}^{(211)}$	0.229	10	0.0928	0.0294	0.077	10	0.0707	0.0224
$V_{3,1}^{(122)}$	0.178	10	0.0513	0.0162	−0.013	10	0.0448	0.0142
$V_{3,1}^{(221)}$	0.046	10	0.0344	0.0109	0.000	10	0.0378	0.0120
$V_{3,1}^{(212)}$	0.178	10	0.0513	0.0162	−0.013	10	0.0448	0.0142
$V_{3,1}^{(222)}$	0.064	10	0.0186	0.0059	−0.007	10	0.0186	0.0059

pair ECI's, we use an approximate prototype result for phase separation on the bcc lattice at $c=0.5$:[55] $kT/8V_{\text{NN}}\approx 0.80$. With this result, it can be seen that the transition temperature for the W-Cr binary edge that we will obtain using the ECI's from SK(I) is close to 16 000 K, clearly an unphysical result. The transition for W-Cr using SK(II) will be approximately 2600 K, in much better agreement with experiment. CVM calculations using the SK(II) interactions confirm these approximate results. In Sec. II C, we will attempt to address why the results for SK(I) are so unreasonable.

As a final assessment of the ECI's for SK(I) and SK(II), the formation energies of disordered $W_xMo_yCr_{1-x-y}$ al-

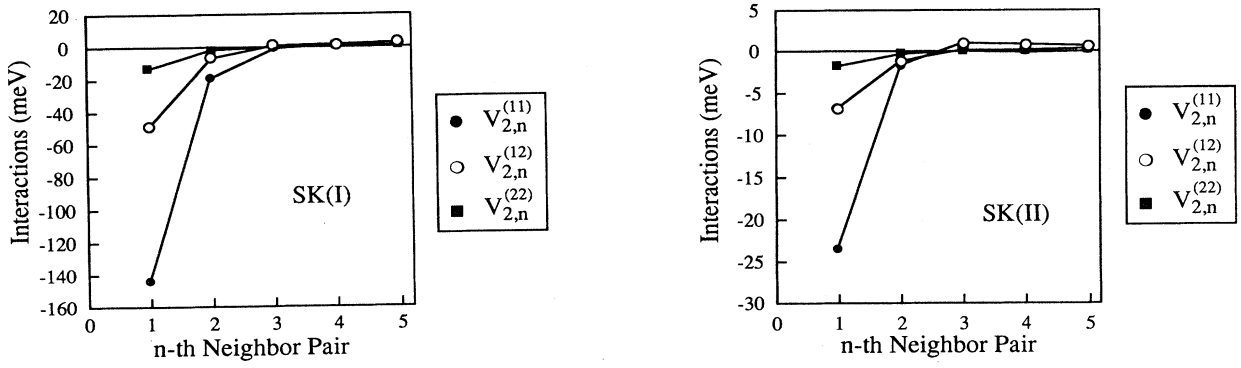

FIG. 2. Pair interactions (in meV) for W-Mo-Cr as a function of separation for the two sets of Slater-Koster parameters given in Table II [SK(I) and SK(II)]. Legends indicate the three types of interactions for each pair. In both cases, the interactions decay rapidly with respect to pair separation; for $n>2$, all interactions can be neglected. The values for $V_{2,n}^{(12)}$ are those for $V_{2,n}^{(12+21)}$ from Table II divided by two.

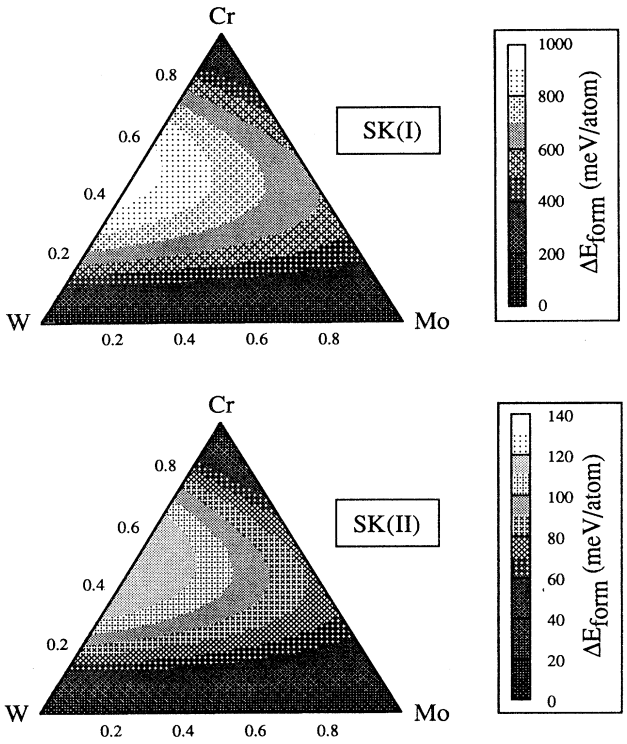

FIG. 3. Energies of formation as a function of concentration for disordered $W_xMo_yCr_{1-x-y}$ alloys for SK(I) and SK(II). Positive formation energies indicate phase separation to be favored for all alloy compositions. Formation energies on the W-Cr and W-Mo binary edges appear to be symmetric, while there is a slight asymmetry in Mo-Cr formation energies. The qualitative features of the formation energy surface do not change much between SK(I) and SK(II).

loys are calculated using the ECI's in Table IV. The formation energy of a disordered alloy at concentration (c_B,c_C) is given by

$$\Delta E_{\text{form}}(c_B,c_C)=E_{\text{random}}(c_B,c_C) -(1-c_B-c_C)E_A-c_BE_B-c_CE_c\ , \quad (10)$$

where $E_{\text{random}}(c_B,c_C)$ is the energy of the completely disordered state computed using Eq. (3) with ECI's from Table IV and LACF written as a product of point correlation functions determined at the given composition.[26] The formation energy for disordered alloys as a function of composition is plotted is Fig. 3 using ECI's from SK(I) and SK(II). At all compositions and for both SK(I) and SK(II), the formation energy of the disordered state is positive, indicating the fact that a mixture of the pure elements is more stable at $T=0$ K than a disordered alloy (i.e., the system shows clustering tendencies). The difference is minimal between the topology of formation energies predicted with SK(I) and SK(II); it appears that the formation energies for SK(I) are roughly seven times those for SK(II). The formation energy also appears to show a slight asymmetry on the Mo-Cr binary edge, while the other two edges are essentially symmetric. Table V contains formation energies at several different compositions for the binary alloys and experimental results for the same where information is available. The Mo-Cr system appears to be the only system for which there is an experimental heat of formation,[56] and the agreement between the formation energy predicted with SK(II) and experiment is excellent. In general, from Fig. 3 and Table V, it is seen that SK(I) predicts formation energies that are significantly larger than those computed with SK(II). This simply supports the conclusions obtained with the pseudobinary interactions above: SK(I) predicts the system to phase separate much more strongly than SK(II).

B. Cluster-variation-method calculations

The ECI's based on SK(II) are used to compute the solid portion of the W-Mo-Cr phase diagram. The ground-state search confirmed that only the pure elements are ground states for the given set of ECI's; hence CVM calculations only need to treat the disordered bcc phase, since this is the only phase that will appear at finite temperature. Since all of the significant interactions from the DCA calculations are on clusters within the bcc tetrahedron ($V_{2,1}^{(ij)}$, $V_{2,2}^{(ij)}$, $V_{3,1}^{(ij)}$), it is acceptable to perform CVM calculations in the bcc tetrahedron approximation to the entropy. All CVM calculations are performed using the $(1,\sigma,\sigma^2)$ basis set for simplicity; hence the DCA interactions are transformed into this basis set (see Refs. 26 and 29 for the methodology). The usage of $(1,\sigma,\sigma^2)$ simplifies the calculations for two reasons: the V matrix [Eq. (9)] contains only integers in this representation, and the correlation functions are on the interval $[-1,1]$. In a Chebychev formulation, for example, the V-matrix entries would contain real (irrational) numbers and the

TABLE V. Energies of formation for binary and ternary random $W_xMo_yCr_{1-x-y}$ alloys for Slater-Koster sets I and II. All enthalpies are given in meV/atom. In general, formation energies for SK(I) are larger than those for SK(II). Experimental results for $Mo_{0.50}Cr_{0.50}$ are indicated; no data was available for the other alloys considered.

	ΔH_f (random)			
	$Mo_{0.50}Cr_{0.50}$	$W_{0.50}Cr_{0.50}$	$W_{0.50}Mo_{0.50}$	$W_{0.33}Mo_{0.33}Cr_{0.33}$
SK(I)	+605	+954	+23.3	+706
SK(II)	+78.0	+128	+4.58	+93.3
Expt.	+74.8[a]			

[a]Reference 55.

correlation functions would be bounded on an interval between two real numbers. A free energy is constructed with 12 symmetry-distinct DCA interactions (numbers 4–15 in Table III) and is then minimized with respect to all 21 symmetry-distinct correlation functions given in Table III. Effective cluster interactions are not computed as a function of volume; hence the CVM calculations are volume independent. Calculations are performed in a mixed ensemble, where one chemical potential and one composition are held fixed; this facilitates construction of the phase diagram using intersections of the grand potential.[17,18]

Isothermal sections for a series of temperatures are given in Fig. 4; these sections are grouped together into a three-dimensional diagram in Fig. 5. At the highest temperature (2700 K), the miscibility gap (MG) of the W-Mo-Cr edge begins to penetrate into the Gibbs triangle. As the temperature is progressively decreased, the two-phase field enlarges; tie lines within the two-phase field are seen to rotate towards the Mo-Cr binary edge, indicative of the fact that this will be the next MG encountered. At a temperature of roughly 1750 K, the critical temperature for the Mo-Cr binary is reached, and the system begins to phase separate along this binary edge as well. As the temperature is decreased more, the two-phase field simply continues to enlarge, and at the lowest temperature shown (1400 K), there is almost no solubility in the Gibbs triangle. Phase separation is never seen to occur along the W-Mo binary edge; convergence difficulties with the CVM at very low temperature prevented an absolute determination of the MG transition temperature, although it should definitely exist, since there is a finite tendency towards phase separation along this edge. An estimate using the previously mentioned prototype result ($kT_c/8V_{NN}=0.8$) yields a transition temperature of roughly 120 K for the W-Mo edge.

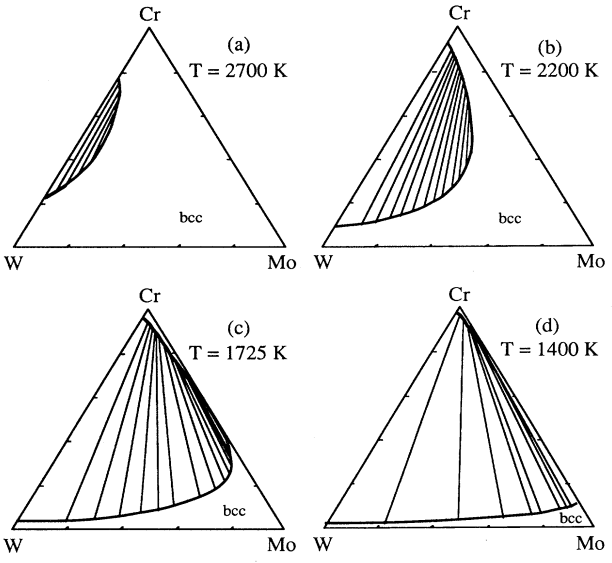

FIG. 4. Isothermal sections of the W-Mo-Cr phase diagram computed within the bcc tetrahedron approximation to the cluster variation method. Each two-phase field is enclosed by bold phase boundary; tie lines are indicated across two-phase fields, and the location of the bcc solid solution is also given. Phase separation occurs in the W-Cr binary first at roughly 2750 K. As the temperature is lowered, the two-phase field grows and the tie lines rotate from the W-Cr edge towards the Mo-Cr in anticipation of the Mo-Cr transition temperature at roughly 1750 K. At 1400 K, the system is essentially completely immiscible except for a small region of Cr deficient solid solution. A slight asymmetry can be seen in the limiting Mo-Cr binary miscibility gap, whereas the W-Cr miscibility gap appears completely symmetric.

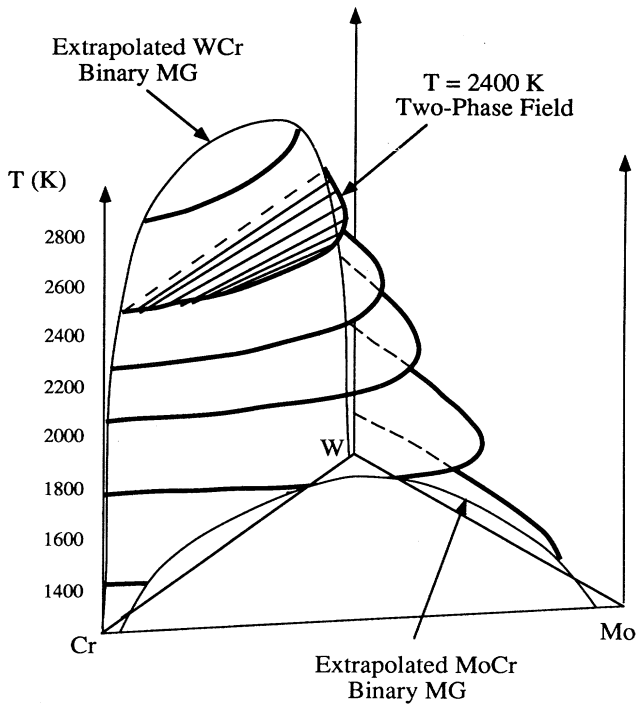

FIG. 5. Complete three-dimensional ternary phase diagram for the W-Mo-Cr system computed within the bcc tetrahedron approximation of the CVM using *ab initio* effective cluster interactions. Each bold curve represents a phase boundary within an isothermal section; tie lines are only included in the 2400-K section for illustrative purposes. Limiting W-Cr and Mo-Cr binary miscibility gaps are indicated.

The behavior shown in Figs. 4 and 5 for the phase equilibria in this system seems to be consistent with intuition for how W-Mo-Cr should behave (see Sec. II C). One nice feature that the calculations seem to predict is the (a)symmetry present in the binary W-Cr and Mo-Cr phase diagrams, a feature one might expect based on the observed asymmetry in the formation energy of disordered alloys (Fig. 3). Experimentally, W-Cr exhibits an almost completely symmetric MG, while there is an asymmetry in solubility in the Mo-Cr system of approximately 5% (Mo is more soluble in Cr than vice versa). The limiting behavior for W-Cr in Fig. 5 seems to be completely symmetric, while that for Mo-Cr shows a slight symmetry in the correct direction. The asymmetry is most apparent in the isothermal section for $T=1725$ K [Fig. 4(d)]. In binary systems, if one uses only

concentration-independent pair interactions, it is impossible to produce a phase diagram that is asymmetric around $c=0.5$, i.e., the multiplet interactions are completely responsible for any asymmetry. The same will be true for the binary edges that comprise a ternary system, hence the small triplet interactions given in Table III (and included in the calculation) seem to be necessary to reproduce the asymmetry observed experimentally. The main shortcoming of these calculations is that the transition temperatures for the W-Cr and Mo-Cr edges are predicted to be roughly 800 and 600 K higher than the experimental results for W-Cr and Mo-Cr, respectively.

C. Discussion

The topology of the predicted W-Mo-Cr phase diagram is pleasingly consistent with intuition for this particular system (no experimental results exist for comparison). Since the W-Cr and Mo-Cr binary edges strongly exhibit phase separation, one expects that addition of a small amount of the third component (Mo and W, respectively) should not alter the phase behavior significantly. Thus, solid solutions of all three components should exhibit phase separation over a range of compositions in the Gibbs triangle. Addition of the third component will either raise or lower the MG transition temperature relative to the binary edge depending on the relative magnitude of the ordering tendencies between the three pairs of elements.[57,58] In the present case, the addition of Mo to W-Cr lowers the MG temperature as Mo is added to W-Cr (no island MG is formed in the center of the Gibbs triangle). Below the binary W-Cr MG maximum, the system will start to phase separate for finite concentrations of Mo. As the temperature is decreased further, the tendency for Mo and Cr to phase separate becomes more important, and the MG extends further away from the W-Cr binary edge. Finally, at the critical temperature for phase separation in Mo-Cr, the two-phase field connects with the Mo-Cr binary edge. The two-phase field widens as the temperature is lowered, indicating the cumulative effects of clustering tendencies in W- and Mo-Cr. Eventually, we expect a reaction on the W-Mo binary edge, which should intrude into the Gibbs triangle, creating a three-phase equilibria between W, Mo, and Cr. This three-phase equilibria will ultimately yield phase separation between the pure elements in the limit of zero temperature. The latter three-phase equilibria is not observed in the CVM calculations since it is not possible to probe low enough temperatures. Regardless, all of the CVM calculations are consistent with what we would expect in a system that contains three binary MG's with the relative transition temperatures observed in this analysis. It is also what has been partially observed in ternary fcc prototype studies using NN pair interactions that produce the same ground states.[17]

It seems that the primary objection that might be raised to these results would concern the overestimates of the transition temperatures for the limiting binary edges (and presumably for phase separation away from the edges as well). While it is commonplace for mean-field calculations to overestimate transition temperatures by roughly 5–10 %, the error in the present case is excessive. The calculations are done without including any effects of volume relaxation on the free energy, a severe approximation in a system that has such a large size mismatch between the elements. The importance of treating elastic relaxations has been demonstrated to be important in binary systems,[59–61] and the same will hold for ternary systems. Hence, we expect that the results could be improved if either a set of volume-dependent interactions is used (discussed below) or some other correction is made to address the issues of elastic relaxation in the disordered phase. Vibrational effects on the free energy, which are neglected, could also be significant in this system,[61,62] but no attempt will be made here to address this issue in any depth.

An issue that is related to the question of volume relaxation is that concerning the choice of Slater-Koster parameters for the DCA calculation. The interactions computed using the two different sets of SK parameters are vastly different, and it is natural to ask why this is the case. To address this question, it is useful to discuss general trends observed in tight-binding descriptions of ordering in alloys. Many TB calculations of properties of binary transition-metal alloys involve d-band-only computations, where the pure-element hopping integrals are all assumed to be equal to canonical values (a "canonical d-band" calculation), i.e., there is no off-diagonal disorder (ODD) in the electronic Hamiltonian. ODD is basically a measure of how strongly the configuration of atoms in the system (i.e., ordered or disordered) affects the off-diagonal matrix elements of the Hamiltonian (hopping integrals between unlike atoms, in the case of TB). If the off-diagonal matrix elements are configuration independent, then there is no ODD. In canonical d-band calculations for binary phase diagrams,[63] the ordering tendencies are only based on the number of d electrons that each element possesses.[2,25] If the two elements have the same number of d electrons, then a canonical d-band calculation would predict no tendency towards ordering or phase separation. Ducastelle[2] showed with some simple arguments concerning the moments of the density of states that when ODD is present, the tendency for ordering (phase separation) is always reduced (enhanced). Since W, Mo, and Cr possess the same number of d electrons, a canonical d-band calculation would predict no ordering tendency in any of the binaries. Thus, if any ODD is present in the Hamiltonians for the three binary alloys, the systems should phase separate, since ODD *always* enhances this tendency.

A common measure of the ODD for transition-metal alloys is the ratio of the d-band widths of the two elements (δ_{BW}), each of which (in d-band-only calculations) is proportional to the NN $dd\sigma$ hopping integral for that element.[25] We define an ODD parameter as the ratio of the *NN* $dd\sigma$ hopping integrals: $\delta_{BW}(I-J)=dd\sigma(I)/dd\sigma(J)$, where $\delta_{BW}=1$ corresponds to no ODD. Using the values for the NN $dd\sigma(I)$ from Table II, one finds for both SK(I) and SK(II) that there is ODD ($\delta_{BW}\neq 1$) for W-Cr, Mo-Cr, and W-Mo with δ_{BW}(W-Cr) $>\delta_{BW}$(Mo-Cr) $>\delta_{BW}$ (W-Mo). Thus, for this system, we

would predict phase separation for all three binary systems with the tendency towards phase separation in binary I-J proportional to $\delta_{BW}(I-J)$. In addition, all ODD parameters for SK(I) are larger than those of SK(II), indicating a stronger driving force for phase separation in the former. Both of these predictions are borne out by the results presented in Sec. II A: NN pseudobinary pair ECI's follow the trend $|W_{pp'}^{W\text{-}Cr}| > |W_{pp'}^{Mo\text{-}Cr}| > |W_{pp'}^{W\text{-}Mo}|$, with results for SK(I) larger in magnitude than those of SK(II).

The difference in ODD between SK(I) and SK(II) can easily be rationalized by considering the effects of changes in volume on the respective d-band widths ($dd\sigma$ elements). In the set SK(I), we have used elements based on the equiatomic volume given by Vegard's law and have thus compressed (expanded) W and Mo (Cr). In doing so, we increase (decrease) the respective d-band widths and $dd\sigma$ hopping parameters, and thus increase the magnitude of the ODD parameter (δ_{BW}). In the case of set SK(II), we use the elements at their equilibrium volumes; hence no alteration in bandwidth of the pure elements occurs, and the ODD is smaller. In both cases, the ODD for W-Mo is small because these elements have almost identical equilibrium volumes. In general, it seems that minimizing the amount of ODD in systems is the best course of action when performing calculations with the DCA, and this is what is done in the calculation of the W-Mo-Cr phase diagram.

The choice of set SK(II) is essentially a way of trying to minimize the deleterious effects that size mismatch has on the calculations. There is another course of action, which involves computing ECI's as a function of volume and performing volume-dependent CVM calculations. In order to compute volume-dependent interactions there are several possible methods, which could be used. The first method one could use is the DCA: one would need to do several LMTO calculations, each at a different volume, then perform the TB-LMTO transformation to obtain interactions at each volume. Such a procedure was employed with success for the Pd-Rh system by Wolverton, de Fontaine, and Dreyssé.[64] If a TB representation is not well suited to the system at hand, then the DCA would not be the best method for computing such a set of ECI's.

If one wished to avoid the use of TB altogether, then one could compute volume-dependent or -independent ECI's using the structure inversion method (SIM).[3,34,65] The only drawback to using this approach in ternary systems is that often a large number of total-energy calculations are necessary to obtain a well-converged set of interactions. Consider the present case of the bcc tetrahedron approximation with only empty, point, pair, and triplet interactions (a total of 15 ECI's). In order to compute this set of ECI's using the SIM, total energies must be computed for a *minimum* of 15 structures. In reality, it would most likely be necessary to include at least 20 structures or more. Such calculations have, in fact, been performed, but the large size mismatch seems to create problems in the LMTO-ASA calculations. If one chooses equal sphere radii for W, Mo, and Cr in the ASA, then there is a large amount of charge transfer. If one modifies the sphere sizes to achieve a charge neutral state, then the total energy changes by 1–4 mRy/atom depending on the sphere sizes. The dependence of total energy on sphere size varies significantly from structure to structure, hence structural energy differences are not a unique function of sphere radii. In general, the LMTO-ASA formation enthalpies are found to vary by up to 100% as a function of sphere radii, and thus it seems that a multiplicity of answers are possible. This problem might be ameliorated by the use of full-potential LMTO (FLMTO) calculations,[66] which is of course even more problematic when one considers the number of structural energies which need to be computed.

Finally, some commentary is needed about the results of Hawkins, Robbins, and Sanchez[46] and Sigli, Kosugi, and Sanchez[47] (hereafter referred to as HRS and SKS, respectively) and what bearing these studies have on the present analysis. HRS computed the phase diagrams for *binary* W-Cr, W-Mo, and Mo-Cr alloys using the tight-binding cluster-Bethe-lattice method (CBLM) in conjunction with the CVM (no ternary alloy properties were considered). The study of SKS included a CVM analysis of the binary Mo-Cr phase diagram, with ECI's that were computed within a TB framework that utilized the coherent potential approximation[67] (CPA) in conjunction with the generalized perturbation method (GPM).[3] SKS also included an *ad hoc* vibrational entropy correction to the free energy to reproduce the experimental results. The studies of HRS and SKS presented results that were in better accord with experiment than the present analysis. For example, in the Mo-Cr system, the critical temperatures for phase separation are 1153, 800, 1050, and 1750 K as given by experiment, HRS, SKS, and the present study. The differences between the predictions made by these studies makes it interesting to compare and contrast the methodology (both in the electronic structure and statistical mechanics) used by HRS, SKS, and that used here. All three sets of calculations utilize the bcc tetrahedron approximation of the CVM, an approximation known to be quite accurate compared to more "exact" methods such as Monte Carlo simulation.[55] Given the equivalence in the levels of statistical-mechanical approximation, it is clear that this is not the source of discrepancy between the studies. We therefore turn to an examination of the differences in the treatment of electronic structure (HRS and SKS) and vibrational entropy (SKS only). We begin with a discussion of HRS and their treatment of the electronic structure of the alloy.

The CBLM used in HRS treats the electronic structure of the alloy in a mean-field approach, and also approximates the geometry of the lattice with a single coordination number. In contrast, the DCA not only treats the geometrical aspects of the alloy problem correctly, but also provides a non-mean-field description of disordered alloys in which configurational averages are taken for the appropriate physical quantities. Since the DCA provides, in principle, a more accurate description of the alloy problem than the CBLM, one must consider the practical details of the electronic structure used in both approaches. The present work relies on a TB approxima-

tion, as does HRS, and this leads naturally to an examination of the parameters that enter into the alloy Hamiltonian: the hopping integrals and on-site energies.

The hopping parameters used by HRS were taken from Harrison,[68] where hopping integrals are based on pure elements at their *equilibrium* lattice constants. Hence, these parameters are comparable to the SK(II) hopping integrals contained in Table II, which were found to give the best representation of W-Mo-Cr alloy thermodynamics (Sec. II A). The hopping parameters in HRS show numerical differences with the SK(II) integrals (10–40 %). Both the study of HRS and the present approach show similar differences with the two-center hopping integrals found in Papaconstantopoulos,[69] hence the difference in hopping parameters between HRS and SK(II) does not seem to be unreasonable. The more important fact about the hopping integrals is that those in HRS and SK(II) both possess roughly the same amount of ODD: $dd\sigma(\mathrm{W})/dd\sigma(\mathrm{Cr})=1.78$, 1.67, and 1.91 for HRS, SK(II), and Papaconstantopoulos, respectively. Given the qualitative agreement between these three sets of hopping integrals, these parameters do not seem to be the source of discrepancy. The only possible source of discrepancy in terms of the hopping integrals lies in the fact that HRS considered only $s+d$ electrons, whereas the present analysis uses $s+p+d$ electrons. A comparison of the on-site energies between HRS and the present analysis is difficult, since these authors included phenomenological Coulombic terms in their TB Hamiltonian. HRS incorporate effects due to repulsion (i.e., the ion-ion minus double-counting terms in the Hamiltonian) into the on-site energies via these Coulomb terms.

The TB-CPA-GPM analysis of SKS (Mo-Cr only) used a basis of d orbitals with hopping integrals determined using canonical SK parameters according to the prescription of Harrison[68] (presumably quite similar to those used in HRS). These authors included the important effects of ODD in their analysis, and the CPA treatment of the electronic structure in SKS does not make the severe topological approximations of the CBLM. On-site energies were determined self-consistently using atomic on-site energies shifted by a direct-exchange Coulomb term (similar in spirit to that used in HRS), the value of which seems to have been arbitrarily fixed. An examination of the dominant NN pair interaction in SKS, HRS, and the present study shows the NN EPI in SKS (-16 meV) to be twice the magnitude of that in HRS, and only 25% smaller than that found using SK(II) in this analysis (-20 meV). Without the empirical correction for vibrational entropy included in SKS, their interactions should lead to a transition of roughly 1250 K (again utilizing $kT_c/V_{\mathrm{NN}}\approx 0.80$ from de Fontaine), much higher than the 800 K predicted by HRS for Mo-Cr. This high transition is lowered by fitting a large vibrational entropy correction (roughly 25% of the formation enthalpy at 1500 K) to yield the experimental result. This large correction [which amounts to a shift in T_c (Mo-Cr) of roughly 200 K] was necessary in SKS in order to obtain a close fit with the experimental phase diagram.

In summary, there are several considerations that most likely lead to the different predictions made in HRS, SKS, and the present analysis. The neglect of s and/or p orbitals in the studies of HRS and SKS is a contributing factor, although this effect is most likely small. The dominant effect that differentiates the EPI's predicted by HRS, SKS, and the present study appears to be the phenomenological Coulombic terms in the Hamiltonian's of HRS and SKS. The DCA is based solely on the one-electron contributions to the Hamiltonian with the on-site energies shifted so as to guarantee local neutrality on average. This choice of on-site energies should, however, minimize errors associated with neglecting Coulombic terms in the Hamiltonian. In alloys that possess large size mismatch, such as W-Cr or Mo-Cr, it may be that explicit inclusion of repulsive corrections to the Hamiltonian is necessary, regardless of whether these terms are obtained phenomenologically or otherwise. Both HRS and SKS present phase diagrams that are in good agreement with experiment, although this does not make these studies unqualified successes. SKS *must* include a large vibrational entropy correction (obtained by fitting experimental results) to achieve good agreement with experiment. HRS have fairly good agreement *without* this correction, which seems to present a dilemma: inclusion of a large correction in HRS would most likely worsen the agreement with experiment, and omission of this correction in SKS would do the same. In general, it seems that the phase stability of large size-mismatch systems cannot be derived from only a knowledge of the band-structure energy. Corrections need to be added to account for repulsive terms in the TB Hamiltonian, static atomic displacements and/or vibrational contributions to the free energy. Unfortunately, there is no straightforward first-principles prescription for including the former two effects in a TB framework and the latter in the CVM calculations, aside from using phenomenological corrections as in the studies of HRS and SKS.

CONCLUSION

We have performed a calculation of the W-Mo-Cr ternary phase diagram using the cluster variation method in the bcc tetrahedron approximation. The present study uses the cluster expansion formulation of the ternary CVM in conjunction with the use of effective cluster interactions determined using only the atomic numbers of the constituent elements. The CVM calculations are done using effective pair and triplet cluster interactions computed with the DCA based on a TB-LMTO Hamiltonian. The TB transformation is performed using LMTO-ASA calculations for the three pure elements at two different volumes: (1) the volume of an equiatomic alloy given by Vegard's law and (2) the equilibrium volumes of each element. In each case, the ECI's indicate phase separation, although in the former case, the tendency towards phase separation is unreasonably large due to the degree of off-diagonal disorder in the system. In general, it is found that the tendency towards phase separation scales directly with the degree of ODD. However, it appears that changing the off-diagonal disorder only changes the quantitative results for the ECI's, as evidenced by the insensitivity to ODD in the topology of the

disordered alloy formation energies as a function of concentration.

ECI's based on LMTO-ASA calculations at the equilibrium volumes of each element are used to compute the ternary W-Mo-Cr phase diagram. CVM calculations are performed using a set of 21 independent multisite correlation functions; isothermal sections are found at several temperatures, and the complete solid-solid phase diagram is constructed. While the transition temperatures obtained for the phase diagram are higher on the binary edges than experimental data, the correct trends are observed. Phase separation in the Gibbs triangle begins at the binary W-Cr edge, and as the temperature is lowered, the two-phase field grows until it reaches the binary Mo-Cr edge. A continued decrease in temperature simply increases the size of the two-phase field. No phase separation is observed on the W-Mo edge for the temperatures studied. In addition, if the results are extrapolated to the binary edges, they seem to be consistent with the symmetry (asymmetry) observed in the W-Cr (Mo-Cr) binary phase diagrams. This asymmetry is also manifested in the disordered alloy formation energies.

In general, the results obtained are quite encouraging considering the level of approximation used. The large size mismatch in W-Mo-Cr makes some approximations necessary in the computation of TB parameters, yet it is still possible to obtain excellent qualitative results. A more accurate treatment would include the effects of elastic relaxation or vibrational effects on the free energy of the disordered phase, although it is unclear whether such an effort would be justified with respect to changes in the topology of the phase diagram. At any rate, we believe the work in the present paper to be a necessary and important step in nonempirical studies of ternary phase stability. Such an approach to the treatment of ternary alloy phase equilibria has a great deal of potential in terms of theoretical understanding and engineering applications, and will hopefully yield results for more complex systems in the near future.

ACKNOWLEDGMENTS

The authors would like to acknowledge Mark Asta, Marcel Sluiter, and Alphonse Finel for fruitful discussions that related to the present contribution. This work supported by the Director, Office of Basic Energy Sciences, Materials Science Division of the U.S. Department of Energy under Contract Nos. DE-AC03-76SF00098 and DE-AC36-CH10093 and also by the Department of the Army under Contract No. DAAL03-91-G-0268.

[1]D. de Fontaine, Solid State Phys. **47**, 33 (1994).
[2]F. Dusatelle, *Order and Phase Stability in Alloys* (North-Holland, Amsterdam, 1991), Vol. 3.
[3]A. Zunger, in *Statistics and Dynamics of Alloy Phase Transformations, Rhodes, 1993,* edited by P. E. A. Turchi and A. Gonis (Plenum, New York, 1994), p. 361.
[4]R. Kikuchi, Phys. Rev. **81**, 988 (1951).
[5]K. Binder and D. W. Heerman, *Monte-Carlo Simulation in Statistical Physics: An Introduction* (Springer-Verlag, New York, 1988), Vol. 80.
[6]C. Domb, Adv. Phys. **2**, 4715 (1960).
[7]C. Colinet, G. Inden, and R. Kikuchi, Acta Metall. Mater. **41**, 1109 (1993).
[8]A. de Rooy, E. W. van Royen, P. M. Bronsveld, and J. T. M. de Hosson, Acta Metall. **28**, 1339 (1980).
[9]M. Enomoto and H. Harada, Metall. Trans. A **20**, 649 (1989).
[10]M. Enomoto, H. Harada, and M. Yamazaki, CALPHAD **15**, 143 (1991).
[11]R. Kikuchi, J. M. Sanchez, D. de Fontaine, and H. Yamauchi, Acta Metall. **28**, 651 (1980).
[12]G. Rubin and A. Finel, J. Phys. Condens. Matter **5**, 9105 (1993).
[13]H. Yamauchi and D. de Fontaine, in *Computer Modelling of Phase Diagrams,* edited by L. H. Bennett (The Metallurgical Society, Toronto, 1985), p. 67.
[14]N. S. Golosov and A. M. Tolstik, J. Phys. Chem. Solids **35**, 1575 (1974).
[15]N. S. Golosov and A. M. Tolstik, J. Phys. Chem. Solids **35**, 1581 (1974).
[16]N. S. Golosov and A. M. Tolstik, J. Phys. Chem. Solids **37**, 279 (1976).
[17]R. Kikuchi, D. De Fontaine, M. Murakami, and T. Nakamura, Acta Metall. **25**, 207 (1977).
[18]R. Kikuchi, Acta Metall. **25**, 195 (1977).
[19]A. Marty, Y. Calvayrac, F. Guillet, and P. Cénédèse, Phys. Rev. B **44**, 11 640 (1991).
[20]R. Osorio, S. Froyen, and A. Zunger, Phys. Rev. B **43**, 14 055 (1991).
[21]R. Osorio, Z. W. Lu, S.-H. Wei, and A. Zunger, Phys. Rev. B **47**, 9985 (1993).
[22]R. Osorio and S. Froyen, Phys. Rev. B **47**, 1889 (1993).
[23]J. M. Sanchez, in *Structural and Phase Stability of Alloys,* edited by J. L. Moran-Lopez, F. Mejia-Lira, and J. M. Sanchez (Plenum, New York, 1991), p. 151.
[24]J. M. Sanchez, F. Ducastelle, and D. Gratias, Physica **128A**, 334 (1984).
[25]V. Heine, in *Solid State Physics. Advances in Research and Applications* (Academic, New York, 1980), Vol. 35, p. 1.
[26]C. Wolverton and D. de Fontaine, Phys. Rev. B **49**, 8627 (1994).
[27]G. B. Taggart, J. Phys. Chem. Solids **34**, 1917 (1973).
[28]G. Inden and W. Pitsch, in *Materials Science and Technology: A Comprehensive Treatment* (Weinheim, New York, 1991), p. 497.
[29]R. McCormack, G. Ceder, C. Wolverton, and D. de Fontaine, in *Alloy Modeling and Design, Pittsburgh, 1993,* edited by G. M. Stocks and P. E. A. Turchi (The Minerals, Metals & Materials Society, Warrendale, PA, 1994).
[30]L. G. Ferreria, S. Wei, and A. Zunger, Phys. Rev. B **40**, 3197 (1989).
[31]Z. W. Lu, S.-H. Wei, A. Zunger, S. Froa-Pessoa, and L. G. Ferreira, Phys. Rev. B **44**, 512 (1991).

[32]C. Wolverton, M. Asta, H. Dreyssé, and D. de Fontaine, Phys. Rev. B **44**, 4914 (1991).
[33]C. Wolverton, G. Ceder, D. de Fontaine, and H. Dreyssé, Phys. Rev. B **48**, 726 (1993).
[34]J. W. D. Connolly and A. R. Williams, Phys. Rev. B **27**, 5169 (1983).
[35]A. Gonis, X.-G. Zhang, A. J. Freeman, P. Turchi, G. M. Stocks, and D. M. Nicholson, Phys. Rev. B **36**, 4630 (1987).
[36]F. Ducastelle and F. Gautier, J. Phys. F **6**, 2039 (1976).
[37]H. Dreyssé, A. Berera, L. T. Wille, and D. de Fontaine, Phys. Rev. B **39**, 2442 (1989).
[38]O. K. Andersen and O. Jepsen, Phys. Rev. Lett. **53**, 2571 (1984).
[39]M. Asta, C. Wolverton, D. de Fontaine, and H. Dreyssé, Phys. Rev. B **44**, 4907 (1991).
[40]A. Finel, in *Alloy Phase Stability,* edited by G. M. Stocks and A. Gonis (Kluwer, Dordrecht, 1989), p. 29.
[41]D. A. Vul and D. De Fontaine, in *Materials Theory and Modelling,* edited by J. Broughton, P. D. Bristowe, and J. M. Newsam, MRS Symposia Proceedings No. 291 (Materials Research Society, Pittsburgh, 1993), p. 401.
[42]J. M. Sanchez and D. de Fontaine, Phys. Rev. B **17**, 2926 (1978).
[43]M. Sluiter, Comput. Mater. Sci. **2**, 293 (1994).
[44]G. Ceder, G. D. Garbulsky, D. Avis, and K. Fukuda, Phys. Rev. B **49**, 1 (1994).
[45]T. B. Massalski, J. L. Murray, L. H. Bennett, and H. Baker, *Binary Alloy Phase Diagrams* (American Society for Metals, Metals Park, OH, 1986), Vol. 1-2.
[46]R. J. Hawkins, M. O. Robbins, and J. M. Sanchez, Phys. Rev. B **33**, 4782 (1986).
[47]C. Sigli, M. Kosugi, and J. M. Sanchez, Phys. Rev. Lett. **57**(2), 253 (1986).
[48]O. K. Anderson, Phys. Rev. B **12**, 3060 (1975).
[49]J. Chen, D. Singh, and H. Krakauer, Phys. Rev. B **38**, 12 834 (1988).
[50]D. Singh and J. Ashkenazi, Phys. Rev. B **46**, 11 570 (1992).
[51]U. von Barth and L. Hedin, J. Phys. C **5**, 1629 (1972).
[52]H. Shiba, Prog. Theor. Phys. **46**, 77 (1971).
[53]D. de Fontaine, A. Finel, H. Dreyssé, M. Asta, R. McCormack, and C. Wolverton, in *Proceedings of the NATO Advanced Research Workshop on Metallic Alloys: Experimental and Theoretical Perspectives, Boca Raton, 1993,* edited by J. S. Faulkner and R. G. Jordan (Kluwer, Dordrecht, 1994), p. 205.
[54]J. M. Sanchez, Phys. Rev. B **48**, 14 013 (1993).
[55]D. de Fontaine, Solid State Phys. **34**, 73 (1979).
[56]R. Hultgren, P. D. Desai, D. T. Hawkins, M. Gleiser, and K. K. Kelley, *Selected Values of the Thermodynamic Properties of Binary Alloys* (American Society for Metals, Metals Park, Ohio, 1973).
[57]J. L. Meijering, Phillips Res. Rep. **6**, 183 (1951).
[58]J. L. Meijering, Phillips Res. Rep. **5**, 333 (1950).
[59]M. Asta, R. McCormack, and D. de Fontaine, Phys. Rev. B **48**, 748 (1993).
[60]D. B. Laks, L. G. Ferreira, S. Froyen, and A. Zunger, Phys. Rev. B **46**, 12 587 (1992).
[61]J. M. Sanchez, J. P. Stark, and V. L. Moruzzi, Phys. Rev. B **44**, 5411 (1991).
[62]G. D. Garbulsky and G. Ceder, Phys. Rev. B **49**, 6327 (1994).
[63]M. Sluiter, P. Turchi, F. Zezhong, and D. de Fontaine, Phys. Rev. Lett. **60**, 716 (1988).
[64]C. Wolverton, D. de Fontaine, and H. Dreyssé, Phys. Rev. B **48**, 5766 (1993).
[65]M. Asta, D. de Fontaine, and M. Van Schilfgaarde, J. Mater. Res. **8**, 2554 (1993).
[66]M. Methfessel, Phys. Rev. B **38**, 1537 (1988).
[67]P. Soven, Phys. Rev. B **2**, 4715 (1970).
[68]W. A. Harrison, *Electronic Structure and the Properties of Solids* (Dover, New York, 1989).
[69]D. A. Papaconstantopoulos, *Handbook of the Band Structure of Elemental Solids* (Plenum, New York, 1986).